The Astrophysical Journal, 805:11 (11pp), 2015 May 20 doi:10.1088/0004-637X/805/1/11

DIFFERENT DYNAMICAL AGES FOR THE TWO YOUNG AND COEVAL LMC STAR CLUSTERS, NGC 1805 AND NGC 1818, IMPRINTED ON THEIR BINARY POPULATIONS

Aaron M. Geller[1,2,6], Richard de Grijs[3,4], Chengyuan Li[3,4], and Jarrod R. Hurley[5]
[1] Center for Interdisciplinary Exploration and Research in Astrophysics (CIERA) and Department of Physics and Astronomy, Northwestern University, 2145 Sheridan Road, Evanston, IL 60208, USA; a-geller@northwestern.edu
[2] Department of Astronomy and Astrophysics, University of Chicago, 5640 S. Ellis Avenue, Chicago, IL 60637, USA
[3] Kavli Institute for Astronomy and Astrophysics, Peking University, Yi He Yuan Lu 5, Hai Dian District, Beijing 100871, China
[4] Department of Astronomy, Peking University, Yi He Yuan Lu 5, Hai Dian District, Beijing 100871, China
[5] Centre for Astrophysics and Supercomputing, Swinburne University of Technology, VIC 3122, Australia
Received 2015 January 26; accepted 2015 March 15; published 2015 May 13

ABSTRACT

The two Large Magellanic Cloud star clusters, NGC 1805 and NGC 1818, are approximately the same chronological age (∼30 Myr), but show different radial trends in binary frequency. The F-type stars (1.3–2.2 $M_{\odot}$) in NGC 1818 have a binary frequency that decreases toward the core, while the binary frequency for stars of similar mass in NGC 1805 is flat with radius, or perhaps bimodal (with a peak in the core). We show here, through detailed *N*-body modeling, that both clusters could have formed with the same primordial binary frequency and with binary orbital elements and masses drawn from the same distributions (defined from observations of open clusters and the field of our Galaxy). The observed radial trends in binary frequency for both clusters are best matched with models that have initial substructure. Furthermore, both clusters may be evolving along a very similar dynamical sequence, with the key difference that NGC 1805 is dynamically older than NGC 1818. The F-type binaries in NGC 1818 still show evidence of an initial period of rapid dynamical disruptions (which occur preferentially in the core), while NGC 1805 has already begun to recover a higher core binary frequency, owing to mass segregation (which will eventually produce a distribution in binary frequency that rises only toward the core, as is observed in old Milky Way star clusters). This recovery rate increases for higher-mass binaries, and therefore even at one age in one cluster, we predict a similar dynamical sequence in the radial distribution of the binary frequency as a function of binary primary mass.

Key words: binaries: general – galaxies: star clusters: individual (NGC 1805, NGC 1818) – Magellanic Clouds – methods: numerical – stars: kinematics and dynamics

1. INTRODUCTION

Binary, and higher-order multiple, stars are ubiquitous and comprise a relatively large fraction of the stars in star-forming regions (Ghez et al. 1993; Köhler et al. 2000; Kraus et al. 2011; Bate 2012; Sana et al. 2013), open clusters (Mermilliod et al. 1992; Patience et al. 1998, 2002; Geller et al. 2008, 2010; Hole et al. 2009), and the Galactic field (Raghavan et al. 2010). For solar-type stars, the binary frequency[7] in the Galactic field is approximately 50%, while for the most massive stars, the binary frequency increases to about 70% (and perhaps even higher, e.g., Raghavan et al. 2010; Sana et al. 2012; Caballero-Nieves et al. 2014).

Binaries in the Galactic field live essentially in isolation, and only the very widest field binaries (e.g., those with separations over $\sim 10^3$ AU) are in danger of encountering passing stars or having their orbits changed dramatically by the Galactic tidal field (Kaib & Raymond 2014). However, most stars (with masses $\geqslant 0.5\,M_{\odot}$) form in denser environments (Lada & Lada 2003; Evans et al. 2009; Bressert et al. 2010). Though many young, embedded, star clusters quickly dissolve to populate the Galactic field (Adams & Myers 2001), close stellar encounters within these birth environments are capable of significantly modifying the orbits of, and even disrupting, binary systems that would otherwise be stable in the Galactic field. Therefore, our interpretation of the observed binary populations in star clusters and the field, as well as our understanding of star formation in general, relies on how a population of stars and binaries evolves through this more dynamically active early stage in a star cluster.

Within star clusters, binaries are typically discussed as either being "hard" or "soft" (Heggie 1975). Hard binaries have high binding energies relative to the kinetic energies of stars moving throughout the cluster, and therefore encounters tend to make hard binaries more tightly bound, or harder. The converse is true for soft binaries, and indeed an encounter involving a soft binary can completely unbind the system.

Observations of binary populations in young star clusters are very valuable for our understanding of the early phases of star cluster dynamics. Two of the youngest well-populated star clusters that have such observations are the Large Magellanic Cloud (LMC) star clusters NGC 1805 and NGC 1818, both with an age of approximately 30 Myr (de Grijs et al. 2002; Li et al. 2013).[8] For both star clusters, de Grijs et al. (2013) and Li et al. (2013) measure the binary frequency as a function of radius from the cluster center. Interestingly, they find that the

[6] NSF Astronomy and Astrophysics Postdoctoral Fellow.

[7] We follow the usual convention and define the binary frequency as $f_{\rm b} = N_{\rm b}/(N_{\rm s} + N_{\rm b} + \ldots)$, where $N_{\rm b}$ is the number of binaries, $N_{\rm s}$ is the number of single stars, and "…" signifies higher-order multiples.

[8] de Grijs et al. (2002) estimate an age for NGC 1805 of $\log(t\,[{\rm yr}]) = 7.00^{+0.30}_{-0.10}$ and for NGC 1818 of $7.40^{+0.30}_{-0.10}$ (from a thorough review of the prior literature), while Li et al. (2013) find an age for NGC 1805 of $\log(t[{\rm yr}]) = 7.65 \pm 0.10$ and for NGC 1818 of 7.25 ± 0.10. This slight disagreement in the cluster ages is likely a result of improved isochrones (and better field star decontamination) employed by Li et al. (2013). For our modeling, we use a single age of 30 Myr for both clusters, which is well within a 3σ confidence interval from each of these age estimates.

two clusters show different trends, where the radial distribution of the binary frequency in NGC 1818 decreases toward the cluster core, and the distribution in NGC 1805 is flat or perhaps bimodal (with a peak in the core).

Their result for NGC 1818 is particularly interesting because, typically, the binary frequencies of star clusters are observed to have the opposite radial trend, increasing toward the core of the cluster (e.g., Geller & Mathieu 2012; Milone et al. 2012). This phenomenon is understood to be a result of mass segregation, where, in a sample containing binaries with primary stars of similar masses to the single stars, the more massive binaries sink toward the cluster center, due to two-body relaxation and dynamical friction.

In Geller et al. (2013b), we studied NGC 1818 in detail through *N*-body modeling. We found that, for a cluster born with soft binaries and no radial dependence of the binary frequency, the observed trend of the binary frequency decreasing toward the cluster core can be naturally explained through the early disruption of wide binaries by close encounters with other stars (on approximately a crossing time). This process occurs preferentially toward the denser core of the cluster, which explains the lower binary frequency in the core relative to the halo. Over a few relaxation times, the binary frequency evolves under the influence of mass-segregation effects, to produce a bimodal radial distribution, and eventually a distribution that rises only toward the core (as is often observed in older star clusters).

The observed bimodal-like radial trend in binary frequency for NGC 1805 (Li et al. 2013) is similar to the second phase in this evolutionary sequence, where mass-segregation effects begin to become important for determining the radial distribution of the binary frequency. However, NGC 1805 and NGC 1818 are approximately the same chronological age, and furthermore, our models of NGC 1818 suggest that even taking the extremes of the age range from de Grijs et al. (2002, and references therein) and Li et al. (2013), cannot alone explain the differences in their binary frequency radial distributions (with all else being equal between the clusters).

The two key differences between these clusters, from a dynamical evolution perspective, is that NGC 1805 is less massive and more centrally concentrated than NGC 1818. Mackey & Gilmore (2003) estimate that NGC 1805 and NGC 1818 have masses of $\log(M/M_{\odot}) = 3.52 \pm 0.13$ and $4.13^{+0.15}_{-0.14}$, respectively, and core radii of 1.33 ± 0.06 pc and 2.45 ± 0.09 pc, respectively. Consequently, de Grijs et al. (2002) estimate that the current half-mass relaxation time in NGC 1805 is four to five times shorter than in NGC 1818 (de Grijs et al. 2002).

Here we use *N*-body modeling to investigate whether the observations of both NGC 1805 and NGC 1818 can be reproduced with similar initial binary populations, all undergoing the evolutionary sequence discussed in Geller et al. (2013b). If so, this may suggest that binaries can form with similar properties across different environments in the LMC, as is also discussed in Geller et al. (2013a) in the context of open clusters and the field in our Galaxy.

We briefly discuss the setup of our simulations in Section 2. In Section 3, we compare the models directly to the observations of NGC 1805. We then expand upon the analysis of Geller et al. (2013b) and study the evolution of the binary frequency as a function of binary primary-star mass in Section 4. We offer our explanation of the different observed trends in the radial dependence of the binary frequency in NGC 1805 and NGC 1818 through comparisons to our *N*-body models in Section 5. Finally, in Sections 6 and 7, we provide a brief discussion and conclusions.

2. *N*-BODY SIMULATIONS

We perform a modest grid of direct *N*-body simulations using the NBODY6 code (Aarseth 2003) targeted at reproducing the observed surface density profile of NGC 1805 from Mackey & Gilmore (2003) at an age of 30 Myr. Our modeling procedure here is nearly identical to that of Geller et al. (2013a, 2013b), and therefore we point the reader to those papers for additional details not discussed here.

We stress that the initial conditions for the binary populations in these NGC 1805 models are nearly identical to those of our NGC 1818 models from Geller et al. (2013b). Moreover, we input a 100% initial binary frequency (independent of stellar mass and radial position), with binary orbital parameters distributed according to observations of solar-type binaries in young open clusters and the Galactic field (e.g., Geller et al. 2010; Raghavan et al. 2010). Most importantly for our later discussion, the initial orbital period distribution is log-normal (as observed for solar-type binaries, with a mean of $\log(P[\mathrm{days}]) = 5.03$ and $\sigma = 2.28$) and extends from periods of about 0.1–10^{10} days. As explained in Geller et al. (2013b, see particularly Figures 3 and 4), and below, many of the very wide (soft) binaries are disrupted quickly by encounters with other stars. The initial orbital eccentricities are drawn from a Gaussian distribution with a mean of $e = 0.38$ with $\sigma = 0.23$, as is observed for solar-type binaries in the young (~150 Myr) open cluster M35 and consistent with similar binaries in the Milky Way field (Geller et al. 2010, 2013a; Raghavan et al. 2010). We draw binary mass ratios from a uniform distribution, but with limits such that the mass ratio is always less than unity and the mass of the secondary star is always greater than 0.1 $M_{\odot}$, which produces a mass-ratio distribution that is approximately of the form $\mathrm{d}N/\mathrm{d}q \propto q^{-0.4}$, within the observed mass range of Li et al. (2013); see Geller et al. (2013b) for further details. The only differences that are imposed on the initial binaries in these NGC 1805 models from our NGC 1818 models arise from the differences in observed cluster masses and structures, as we explain below.

We choose to investigate two different initial virial ratios of $Q = 0.5$ (equilibrium) and $Q = 0.3$ (collapsing), and two different degrees of substructure, using fractal distributions of degrees[9] $D = 3$ (smooth) and $D = 2$ (clumpy). We follow the same procedure as in Geller et al. (2013b) to generate these initial conditions, namely smooth distributions are generated within the NBODY6 code and substructured initial conditions are generated using McLuster (Küpper et al. 2011). In short, to set up the clumpy models, McLuster first defines a fractal distribution of stars within a unit sphere, and then "folds" this distribution with a given density profile. For simplicity, we choose to begin all models with an underlying Plummer density profile (Plummer 1911); substructure is imposed on top of the

[9] We follow Goodwin & Whitworth (2004) and Küpper et al. (2011) to define the degree of substructure with the parameter, D, such that the probability that a given particle will have a nearby "child" is 2^{D-3}, where $D = 3$ produces no substructure and $D < 3$ produces fractal density distributions. We refer the reader to Goodwin & Whitworth (2004) and Küpper et al. (2011) for specific details on the algorithm used by McLuster for defining the initial fractal density distributions.

Plummer model for those simulations with $D = 2$. Thus, all models begin centrally concentrated, as defined by the Plummer scale radius (or equivalently, the virial radius, as discussed below). At an age of 30 Myr in the simulations, our initially substructured models relax to have smooth density distributions (e.g., see Figure 1 of Geller et al. 2013b).

There are likely other potential combinations of initial Q and D that could reproduce the observations of NGC 1805 at an age of 30 Myr. Here we choose to investigate $[Q, D] = [0.5, 3]$ as a baseline model to compare against collapsing ($Q < 0.5$) and substructured ($D < 3$) models. In general, other studies (including our modeling of NGC 1818) have simulated star clusters with Q ranging from about 0.1 to 0.75, where $Q > 0.5$ are initially expanding clusters. Observations suggest that many clusters form with subvirial ($Q < 0.5$) velocities (Peretto et al. 2006; André et al. 2007; Proszkow et al. 2009; Tobin et al. 2009), and therefore we choose to focus on subvirial models and investigate a moderate value of $Q = 0.3$. Likewise, other studies have investigated a range in D, from about one to three. Again, here we choose a moderate value of $D = 2$ for our substructured models. We do not attempt to identify the most probable specific initial values of $[Q, D]$ through our simulations (and indeed this is likely not possible to any relevant precision, given the observations); instead, we investigate for differences between our baseline (smooth, equilibrium) model and modestly subvirial and/or substructured models.

Compared to NGC 1818, NGC 1805 is relatively compact. The (Elson et al. 1987, EFF) profile fit to the observations of NGC 1805 by Mackey & Gilmore (2003) gives $a = 6.84 \pm 0.42$ arcsec (1.66 ± 0.10 pc, using the canonical LMC distance modulus of 18.5, which equates to a scale of 4.116 arcsec pc^{-1}) and $\gamma = 2.81 \pm 0.10$, which can be converted into a King core radius of 1.33 pc. For reference, a similar calculation for NGC 1818 yields a core radius of 2.45 pc. Mackey & Gilmore (2003) found a central surface brightness in NGC 1805 of $\log\mu_0 = 3.49 \pm 0.02\, L_\odot\, \mathrm{pc}^{-2}$ (which implies a central mass surface density of $155 \pm 7\, M_\odot\, \mathrm{pc}^{-2}$, given the mass-to-light ratio of 0.05 adopted by Mackey & Gilmore 2003). The implied total mass of NGC 1805 is then $\log(M/M_\odot) = 3.52 \pm 0.13$. For reference, de Grijs et al. (2002) found a mass of NGC 1805 of $2.8^{+3.0}_{-0.8} \times 10^3$ $M_\odot$, while Johnson et al. (2001) found a somewhat higher mass of 6000 $M_\odot$.

We aim to create a model of NGC 1805 that reasonably matches these parameters at an age of 30 Myr, by adjusting the initial virial radius (or equivalently, the Plummer scale radius) and initial total mass. From comparisons to our previous simulations of other star clusters (Hurley et al. 2005; Geller et al. 2013a, 2013b), we predict that only a small amount of mass loss will occur over the 30 Myr timescale of interest. To begin, we ran a series of trial simulations of NGC 1805 over a grid in initial number of stars and virial radius and determined that starting with 7600 stars, drawn from a Kroupa (2001) initial-mass function (with masses between 0.1 and 50 $M_\odot$) will evolve to be within the observed mass range of NGC 1805 at 30 Myr. This initial number of stars and mass function results in an initial total cluster mass of ~4700 $M_\odot$ (already within the range of masses estimated from the observations of NGC 1805, though toward the high end). The true initial number of stars, and corresponding initial total cluster mass, of NGC 1805 is most likely not exactly what we have chosen, In general, beginning with more stars (with all else being equal) would result in a longer initial half-mass relaxation time, and therefore less rapid dynamical evolution. The opposite is true for a cluster with a lower number of initial stars. As we discuss below, our simulations do indeed reside within the observed mass range of NGC 1805 at an age of 30 Myr, which is sufficient for our purposes.

To determine the initial virial radius for a given model, we compared results from our initial set of trial simulations to the observed surface density profile at an age of 30 Myr. We find that initial virial radii between 4 and 6 pc (or equivalently, Plummer scale radii between 2.36 and 3.53 pc) fit well to the observations at 30 Myr. Specifically, we will present models with initial virial ratios, fractal dimension, and virial radii, $[Q, D, R_V(\mathrm{pc})] = [0.5, 3, 4]$, $[0.5, 2, 4]$, $[0.3, 3, 4]$, $[0.3, 2, 6]$. We do not model the embedded phase of the cluster here and instead begin our simulations at $t = 0$ after gas expulsion and with all stars on the zero-age main sequence. We compare the simulations at 30 Myr to the observations in Section 3.

To simplify our comparison between models of NGC 1805 and NGC 1818, we place these simulations of NGC 1805 in the same orbit around the LMC as we used in Geller et al. (2013b) for the NGC 1818 simulations. Specifically, we start the cluster at 3.3 kpc from the center of a point mass of $10^{10}\, M_\odot$ on a linearized circular orbit. NGC 1805 is observed to be at about 3.86°–4.00°(~3.4–3.5 kpc; Mackey & Gilmore 2003) from the center of the LMC, but little more is known about the cluster's orbit. This, and the very minor effect on the cluster from the LMC tidal field over 30 Myr, suggests that this small difference between the observations and our choice of orbit is unimportant for the present analysis and understanding. We also note that, in addition to both NGC 1805 and NGC 1818 being at a similar distance from the center of the LMC, they are also on the same side of the parent galaxy, and therefore are also affected in a similar manner by the tidal field of the Small Magellanic Cloud (though this minor effect is not modeled here).

We produce 20 simulations at each combination of virial ratio (Q) and fractal dimension (D), drawing from the same initial parameter distributions, but varying the initial random seed in order to address the stochasticity in N-body simulations.[10] In total, we present results from 80 simulations of NGC 1805.

3. COMPARISON BETWEEN OBSERVATIONS AND SIMULATIONS OF NGC 1805

All of the simulations listed in Section 2 evolve to be consistent with the observed total mass, total binary frequency, and surface density profile of NGC 1805 at an age of 30 Myr. As discussed above, NGC 1805 is observed to have a mass between 2000 and 6000 $M_\odot$ (and Mackey & Gilmore 2003 derived a mass between 2450 and 4470 $M_\odot$). At 30 Myr, our models range in mass from about 3838 to 4312 $M_\odot$. Li et al. (2013) found a binary fraction for NGC 1805 between about 32% and 40% for binaries with primary masses between 1.3 and 2.2 $M_\odot$, mass ratios $\geqslant$0.55, and within a radius of 45 arcsec (or about 11 pc at the distance of the LMC) from the cluster center. Within the same observational limits, our simulations

[10] It is a fairly standard practice to run at least 10 simulations, with initial conditions drawn from the same parent distributions, to assess the expected variation among N-body models of a given star cluster (e.g., Parker & Goodwin 2012; Kouwenhoven et al. 2014).

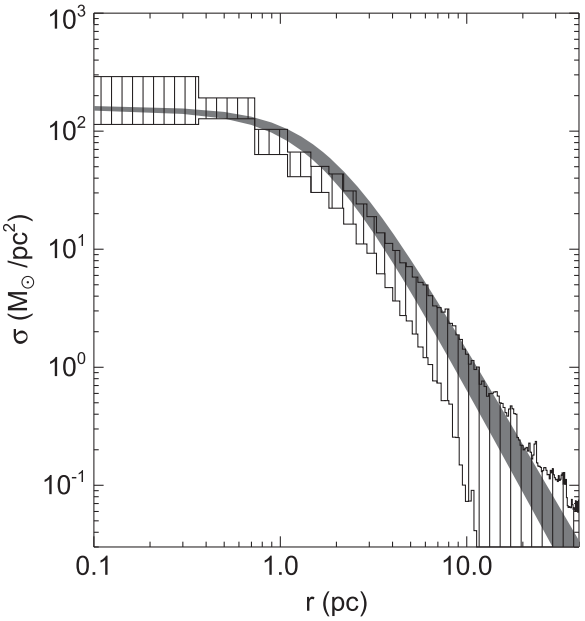

Figure 1. Projected radial mass surface density profile for one NGC 1805 simulation compared to the EFF profile fit to the observations of the cluster by Mackey & Gilmore (2003). We show the same $[Q, D] = [0.5, 2]$ simulation here as in Figure 2, which matches the observed radial distribution of the binary frequency particularly closely. (All of our simulations reproduce the observed surface density profile.) The binned and hatched area shows the region from the simulations within which fall 95% of the 1000 random sight lines. The solid gray band shows the region encompassed by the Mackey & Gilmore (2003) EFF model, with parameters $\log\mu_0 = 3.49 \pm 0.02\ L_\odot\ \mathrm{pc}^{-2}$ ($155 \pm 7\ M_\odot\ \mathrm{pc}^{-2}$), $a = 1.66 \pm 0.10$ pc, $\gamma = 2.81 \pm 0.10$.

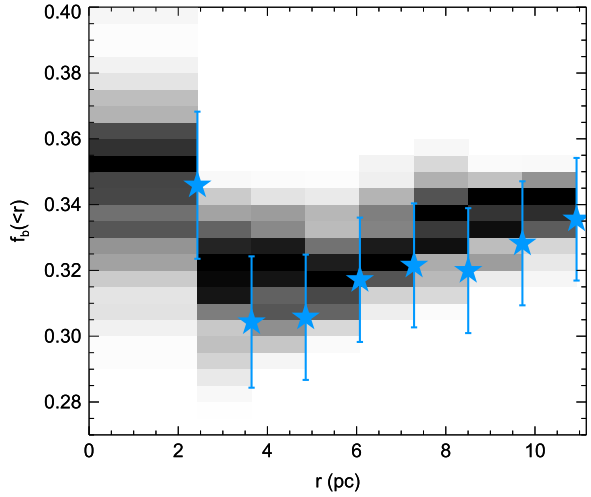

Figure 2. Binary frequency as a function of radius from the cluster center, comparing one NGC 1805 simulation to the observations of Li et al. (2013). For both the observations and the simulation, all single stars and binaries with primary-star masses between 1.3 and 2.2 $M_\odot$ are included. For binaries, we only count those with a mass ratio ($q = m_2/m_1$, where $m_1 > m_2$) $\geqslant$0.55, and each binary with $q < 0.55$ is counted as one single star (due to observational limitations). The observations are shown in colored stars with error bars and indicate the total binary frequency inside the radius where the point is located. In the gray-scale distribution, we show the results from the same $[Q, D] = [0.5, 2]$ simulation as in Figure 1. We use the same cumulative accounting of the binary frequency at the same radial locations as the observations, but for the simulation, we plot the distribution of the binary frequency at each radius resulting from the 1000 different projected sight lines (in bins of $f_b = 0.005$, with darker values indicating higher likelihood). This simulation very closely reproduces the observed bimodal distribution in binary frequency as a function of radius.

have binary frequencies that range from about 21 to 36% (and total binary frequencies between 73 and 82%), at 30 Myr.

In Figure 1, we show one example comparison to the observed surface density profile of NGC 1805 for a particular simulation that also closely matches the observed radial distribution of the binary frequency (see Figure 2). Here, as we will also do throughout the paper when analyzing simulations in projection, we take 1000 different randomly chosen lines of sight through our model and combine the results. Strictly, the orbit of the simulated cluster within the LMC potential defines a true line-of-sight projection for the cluster relative to an observer on Earth. However, given the uncertainties in the true cluster orbital parameters, our simplistic modeling of the LMC potential and random asymmetries within the initial conditions of substructured simulations, we prefer to select many random lines of sight and analyze the resulting distributions as an ensemble. In general, we find that the results (e.g., surface density profile, radial distribution of the binary frequency, etc.) are not particularly sensitive to the specific choice of projection.

We also provide summary information for our simulations in Table 1, including the initial virial ratio (Q), fractal dimension (D), and virial radius (R_V), the number of simulations with these initial parameters ($N_{\rm sims}$), and the 30 Myr total cluster mass (M_c), central surface density (σ_0(obs), only including stars with V magnitudes <25, approximately the faint limit of observations from Mackey & Gilmore 2003), total binary frequency (f_b(tot)), observable binary frequency (f_b(obs), for stars in the simulations within the observed range of Li et al. 2013, stated above), and the percentage of simulations that match the observed binary frequency radial distribution of Li et al. (2013) to within $\leqslant 3\sigma$ (P_{χ^2}(obs)). For all 30 Myr values of a given $[Q, D]$ pairing, we provide the means from the 20 individual simulations. For M_c and f_b(tot), we also provide the standard error on the mean, while for σ_0(obs) and f_b(obs) we provide the upper and lower limits within which lie 95% of our random sight lines across the 20 simulations.

In Figure 2, we compare the observed radial distribution of the binary frequency from Li et al. (2013) to the same simulation shown in Figure 1. Note the very close agreement in both the binary frequency and radial distribution. Furthermore, this simulation reproduces the bimodal structure of the observed radial distribution of the binary frequency while drawing initial binaries from the *same distributions* as our NGC 1818 model (Geller et al. 2013b), which has a distribution of binary frequency at the same chronological age that falls toward the core. We discuss the reasons for this difference in Section 5.

Looking now at the full grid of NGC 1805 simulations, we compare the observed and simulated radial distributions of the binary frequency through a χ^2 analysis, using the same procedure as in Geller et al. (2013b). For clarity, we repeat the definition here:

$$\chi^2 = \sum_r \frac{\left(f_{\rm e}\left(<r\right) - f_{\rm o}\left(<r\right)\right)^2}{e\left[f_{\rm o}\left(<r\right)\right]^2}, \quad (1)$$

where $f_{\rm e}(<r)$ and $f_{\rm o}(<r)$ are the simulated and observed cumulative binary frequency inside the given radius, respectively, and $e[f_{\rm o}(<r)]$ is the error on the observed cumulative binary frequency at the same radius. We have not constrained

Table 1
Summary Table of *N*-body Simulations

Q	D	R_V (pc)	N_{sims}	M_c ($M_\odot$)	σ_0(obs) ($M_\odot$ pc^{-2})	f_b(tot)	f_b(obs)	P_{χ^2}(obs) (%)
0.5	3	4	20	4092 ± 12	105^{+70}_{-61}	0.7637 ± 0.0023	$0.29^{+0.04}_{-0.04}$	27.840
0.5	2	4	20	4017 ± 16	148^{+109}_{-88}	0.7450 ± 0.0022	$0.30^{+0.04}_{-0.07}$	59.315
0.3	3	4	20	4098 ± 12	121^{+71}_{-60}	0.7578 ± 0.0024	$0.28^{+0.03}_{-0.04}$	34.030
0.3	2	6	20	4099 ± 20	108^{+143}_{-70}	0.8004 ± 0.0024	$0.31^{+0.06}_{-0.08}$	49.610

the simulation results, and therefore we have eight degrees of freedom (one for each bin in Figure 2).

The distributions of these χ^2 values, combining results from each of the 1000 projections for each of the 20 models with a given [Q, D] pairing, are shown in Figure 3. Additionally, we provide the percent of sight lines through these simulations that match the observed radial distribution of the binary frequency to within $\leqslant 3\sigma$ in Table 1. First, we find that the initially substructured simulations ($D = 2$) have a distribution of χ^2 values shifted significantly to lower values than that of the initially smooth simulations ($D = 3$; top panel of Figure 3). A Kolmogorov–Smirnov test comparing these two distributions returns a probability $<10^{-7}$ that the two distributions are drawn from the same parent population. Conversely, the distribution of χ^2 values for the NGC 1805 simulations initially in equilibrium ($Q = 0.5$) cannot be distinguished from that of the initially collapsing simulations ($Q = 0.3$), as shown in the middle panel of Figure 3. Thus we find a preference for substructured initial conditions in our models of NGC 1805 (which we also found for our NGC 1818 models in Geller et al. 2013b).

Interestingly, however, only about half of the simulations reasonably reproduce the observed radial distribution of the binary frequency. The gray vertical line shows the χ^2 value for a 3σ deviation of the simulation from the observations (at $\chi^2_{red} \sim 2.95$). We can consider the ~50% of simulations with higher χ^2 values than this limit to be poor fits to the observations. In general, the models that fail to reproduce the observations do so either because they have a different total binary frequency or a radial distribution of the binary frequency that only decreases toward the core. This second point is in line with the results of Geller et al. (2013b), where we find that, for smooth initial conditions, the simulations require at least one to two half-mass relaxation times to produce a bimodal distribution, and NGC 1805 has only lived through about one half-mass relaxation time, or less (see Section 5).

This may indicate that there exists a more accurate choice of initial [Q, D], or other initial parameters, that best reproduces the observed cluster today. However, our goal here is not to identify the exact initial parameters of the cluster, but to investigate whether both NGC 1805 and NGC 1818 could reasonably have been born with very similar primordial binary populations. We find that we can closely reproduce the observations from a subset of our simulations, and therefore we conclude that the observations of both NGC 1805 and NGC 1818 can be reproduced from simulations beginning from very similar initial conditions (with appropriate modifications to the initial cluster mass and virial radius). In the following section, we step back and examine the overall evolutionary trends of the binaries in our different NGC 1805 models.

4. DEPENDENCE OF THE RADIAL DISTRIBUTION OF THE BINARY FREQUENCY ON STELLAR MASS

We can reproduce the two different trends in the observed radial distribution of the binary frequency in NGC 1805 and NGC 1818 through *N*-body simulations that begin with the same initial binary frequency and binary parameters drawn from the same initial distributions at the same chronological age of 30 Myr. Moreover, we do not need to invoke a different primordial binary population or other changes to the primordial population between these two clusters (other than a difference in initial cluster mass and virial radius) to explain these observations. We begin here to investigate the differences between these two clusters, starting with an analysis of the binary frequency as a function of stellar mass. In Geller et al. (2013b), we investigated the effects of binary disruption, two-body relaxation, and mass segregation as a function of time. Examining the binary sample by stellar mass allows us to probe these effects at one age in the simulation, since higher mass stars are expected to undergo dynamical relaxation processes more quickly than lower mass stars.

We focus on the NGC 1805 simulations with [Q, D] = [0.5, 2], as these models most closely reproduce the observed radial distribution of the binary frequency for the observed mass range (see Figures 2 and 3 and Table 1). We divide the model into mass bins of $0.6\,M_\odot$, approximately the mean stellar mass in the simulation at 30 Myr. At masses greater than 10 times this mean mass, the sample size gets too small to continue this bin size (without very large uncertainties), and we therefore group these highest mass stars together into one bin. (The maximum mass of a star in our simulations at 30 Myr is $\sim 9\,M_\odot$.) Due to the relatively small number of stars in NGC 1805, it is unfortunately not possible to retrieve useful binary frequency radial distributions from the observations as a function of mass, owing to the relatively large statistical uncertainties, and therefore here we only analyze the simulations.

We plot the radial distribution of the binary frequency in different mass bins in Figure 4. Here we do not project the model, and instead use the 3D radial position for each star. We also take all binaries into consideration, rather than limiting to mass ratios $\geqslant 0.55$ as we do for direct comparisons to the Li et al. (2013) observations. Although we do not explicitly impose any differences in the binary population as a function of primary mass, we choose to normalize the results at 30 Myr to those at the start of our simulation to remove any stochastic fluctuations that result from drawing relatively small numbers of binaries from broad distributions (most relevant for the higher-mass bins, which have smaller numbers of binaries).

Focusing on the top panel of Figure 4, we point out two general trends in the binary frequency that clearly vary with mass. First, at an age of 30 Myr, the overall binary frequency

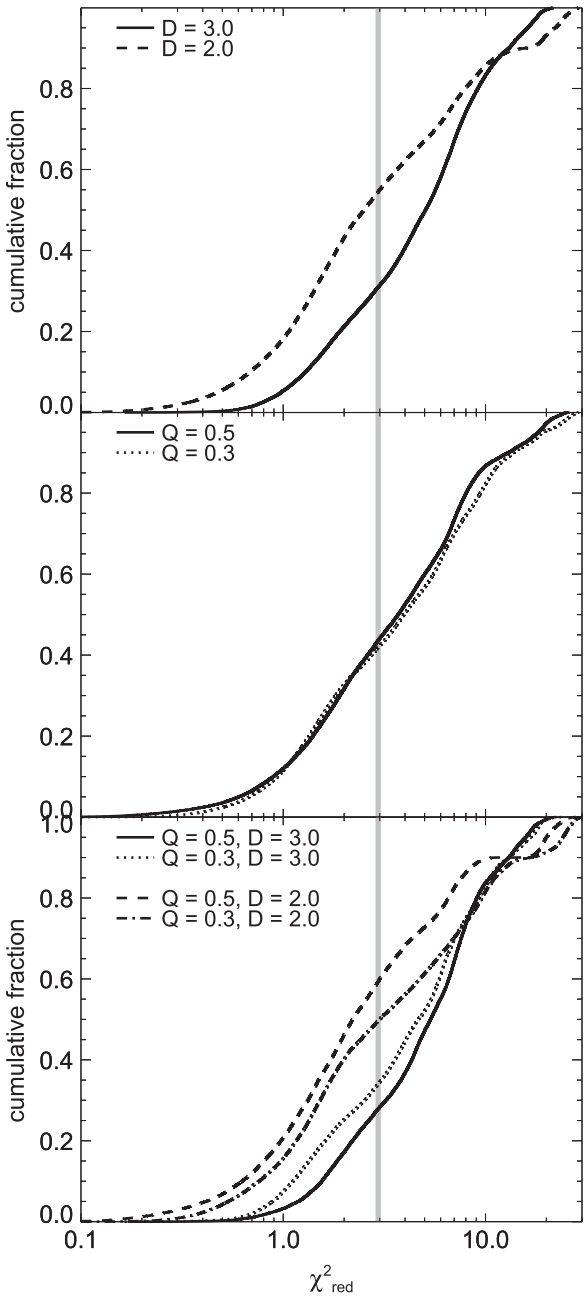

Figure 3. Distribution of χ^2 values comparing the radial distribution of the binary frequency from the NGC 1805 *N*-body simulations to the Li et al. (2013) observations (shown in Figure 2). We define the χ^2 value as in Equation (1) and perform this analysis for all 1000 sight lines to each of our simulations with the given virial ratio (Q) and fractal dimension (D). The top and middle panels each combine the sets of simulations that either have the same fractal dimension (top) or virial ratio (middle), while the bottom panel shows each set of simulations separately. The gray vertical line marks the χ^2 value that indicates a 3σ difference between the observations and simulations (at the given number of degrees of freedom).

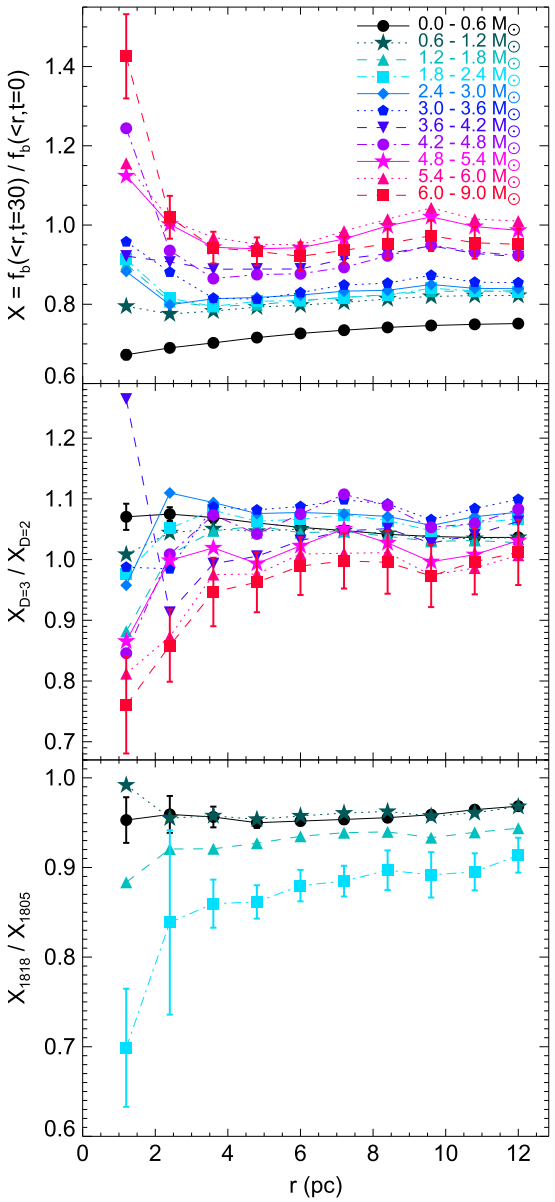

Figure 4. Distributions of binary frequency as a function of radial distance from the cluster center for binaries with different primary-star masses. We cover the same radial domain as the observations, though with a slightly different bin size. Each point represents an analysis of the stars inside the given radius. However, here we do not limit by mass ratio, and we take the three-dimensional radius, rather than projected (as we did in Figure 2 to compare with the observations). Different plotting styles and colors identify the different mass bins and are indicated in the top panel. Each point shows the mean value from each of the 20 simulations for the given [Q, D] pairing. Uncertainties show the standard errors on these means (with error propagation in the plotted ratios). As an indicator of the range in uncertainties from all mass bins, and for ease of viewing, we only show uncertainties for the lowest and highest mass bin (which have approximately a factor of 200 difference in the total number of binaries). In the top panel, we show the binary frequency as a function of radius at 30 Myr (the age of NGC 1805) for our [Q, D] = [0.5, 2] NGC 1805 simulations, the set of simulations that are most consistent with the binary observations (e.g., see Figure 3 and Table 1). We normalize each bin by the value at the start of the simulation to remove any stochastic fluctuations resulting from drawing small numbers of stars from broad distributions in each of the individual simulations. In the middle panel, we plot the ratio of these values to those of our [0.5, 3] NGC 1805 simulations, the set of simulations that are the least consistent with the binary observations. Finally, in the bottom panel we plot the ratio of the values in the top panel to a similar analysis of our NGC 1818 simulations with [Q, D] = [0.5, 2] (the same initial [Q, D] as shown for NGC 1805 in the top panel).

increases toward higher-mass stars. Second, the binaries with higher-mass primaries show more dynamically evolved radial distributions. Furthermore, a χ^2 test comparing the radial distribution of the binary frequency for the lowest-mass binaries to that of any of the other mass bins returns a distinction at very high confidence (>6σ).

This first phenomenon can be understood by also looking at the distributions of semimajor axes for binaries of different

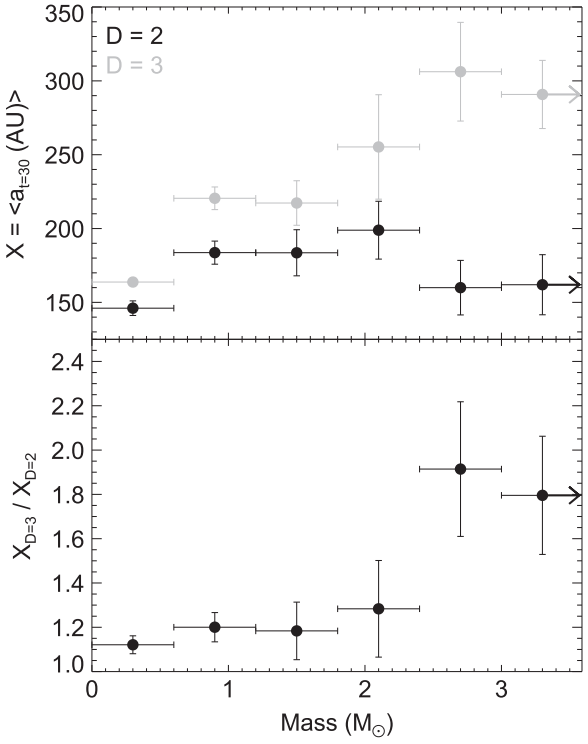

Figure 5. Distributions of mean binary semimajor axis for bins of different binary primary mass, comparing our NGC 1805 simulations with $[Q, D] = [0.5, 2]$ and $[0.5, 3]$ at 30 Myr. We only include binaries with main-sequence primary stars within one initial half-mass radius (~3.07 pc) of the cluster center. The points show the mean values from each of the 20 respective simulations for the given $[Q, D]$ pairing, and the vertical error bars show the standard errors on the means (with error propagation in the bottom panel). The horizontal error bars indicate the bin size; the last bin extends to the most massive stars in the cluster (~9 $M_\odot$), but is truncated here for ease of viewing. In the top panel, we compare the distributions for the two sets of simulations directly (with the $D = 2$ simulations in black and the $D = 3$ simulations in gray). In the bottom panel, we take the ratio of the results from these two simulations.

masses. In the top panel of Figure 5, we show the mean semimajor axis within bins of the primary star's mass for both the $[Q, D] = [0.5, 2]$ and $[0.5, 3]$ models. As discussed in detail in Geller et al. (2013b) and also relevant here, the widest binaries are dynamically disrupted early in the simulations, which accounts for the overall drop in binary frequency seen in Figure 4. Figure 5 shows that the higher-mass binaries survive out to larger separations than the lower-mass binaries (although this is more apparent for the initially smooth model, and we will discuss this difference in Section 4.1). As the semimajor axes for all binaries were drawn from the same (broad log-normal) distribution, this result indicates that a larger frequency of higher-mass binaries than lower-mass binaries are able to survive disruptions by an age of 30 Myr.

The second trend that we point out above may be expected from two-body relaxation timescale arguments. Returning to the top panel of Figure 4 we see that, for instance, the binaries with primary masses less than the mean mass have a binary frequency that decreases toward the core of the cluster. Moving to bins containing higher and higher mass binaries, the distributions increase more and more toward the cluster center and also begin to display a bimodal distribution. We discussed this behavior in detail in Geller et al. (2013b) as a typical trend that a population of binaries may go through *as a function of time*. Here we note that even at one given time, the same trend can be observed by examining binaries of different masses. Moreover, this shifting from a decreasing to increasing trend of binary frequency toward the cluster core depends on the relaxation timescale, which decreases toward higher-mass stars.

4.1. Differences in the Evolution of the Smooth and Substructured Models

Our models with substructured initial conditions ($D = 2$) reproduce the observations more closely than those with smooth initial conditions (see Figure 3 and Table 1). Below, we point out a few key differences between these two sets of simulations that may help to explain the reasons behind this preference. For simplicity, we will focus on the simulations that begin initially in virial equilibrium ($Q = 0.5$).

We start with the middle panel of Figure 4, where we plot the ratio of radial distributions of the binary frequency from the $[Q, D] = [0.5, 3]$ (initially smooth) simulations over that of the $[0.5, 2]$ (initially substructured) simulations. For nearly all mass bins, this ratio decreases toward the cluster core. Moreover, this ratio decreases more strongly toward the core as we consider binaries with higher mass primaries. A χ^2 test distinguishes the distribution for lowest-mass binaries from that of the highest-mass binaries at $>4.5\sigma$ (and at $>3\sigma$ for the highest-mass bin compared to the 0.6–1.2 $M_\odot$ bin, the 1.8–2.4 $M_\odot$ bin, and the 2.4–3.0 $M_\odot$ bin). In other words, at 30 Myr, the binary frequency in the core for a given binary primary mass is lower in the simulations with smooth initial conditions than for those with substructured initial conditions, and this difference is more pronounced for higher-mass binaries.

It may be tempting to conclude that the lower binary frequency at 30 Myr in the core of the initially smooth models is due to the more efficient disruption of binaries in those models, as compared to the initially substructured models. However, turning to Figure 5, where we compare the mean semimajor axes for binaries in bins of increasing primary mass at 30 Myr, we see that in fact the opposite is true. Again, we began all of our simulations by drawing binaries from the same initial distribution of semimajor axes (with no dependence on initial masses) and allow dynamical encounters to naturally disrupt wide binaries. The simulations that begin with initially substructured density distributions are more effective at disrupting binaries, of all primary masses. At an age of 30 Myr, the mean semimajor axis for binaries within one initial half-mass radius ($r_h(0) \sim 3.07$ pc) for the 20 simulations initially with smooth density distributions ($[Q, D] = [0.5, 3]$) is 190 ± 3 AU, compared to the 160 ± 3 AU for the simulations with initially substructured density distributions ($[Q, D] = [0.5, 2]$) within the same radial domain. A Kolmogorov–Smirnov test comparing these two semimajor axis distributions returns a probability of 2×10^{-10} that the two are drawn from the same parent distribution.

This distinction is also seen in the top panel of Figure 5, where the mean semimajor axis in every mass bin for the $[0.5, 3]$ simulation is higher than that of the $[0.5, 2]$ simulation, and in the bottom panel, where the ratio of these values is always greater than one. The bottom panel of Figure 5 also shows that the ratio of the mean semimajor axes for these two sets of simulations is largest for binaries with the highest-mass primaries. This result indicates that in the initially substructured simulations, the higher-mass binaries undergo more energetic encounters than in the initially smooth simulations.

These effects can all be understood under the same physical framework as follows. The initially substructured simulations undergo more rapid relaxation than the initially smooth simulations early in the cluster evolution. This situation physically resembles the conditions of violent relaxation (Lynden-Bell 1967; Elson et al. 1987; Spera & Capuzzo-Dolcetta 2015), where the response of particles to processes like mass segregation is stronger if there are significant gradients in the background potential, which we also have here in the presence of substructure. This causes the higher-mass binaries to segregate more quickly toward the core, producing the effect seen in Figure 4. The result that star clusters with initially substructured density distributions undergo mass segregation more rapidly is well known from *N*-body star cluster models, and was first discussed by McMillan et al. (2007; and soon thereafter by, e.g., Allison et al. 2009 and Moeckel & Bonnell 2009, using more extensive models), as a potential explanation for very young star clusters that are observed to have significant mass segregation, which is inconsistent with expectations from standard two-body relaxation processes (from unsegregated initial conditions). We confirm this result here, now from the viewpoint of binary stars.

Furthermore, because of pockets of initially very high density in the substructured simulations relative to the smooth simulations, the semimajor axis distributions for binaries of all masses are shifted to lower values, by a factor of about 1.2, on average, inside of $r_h(0)$ (see also the top panel of Figure 5). Additionally, the higher-mass binaries in the substructured models segregate toward these high density regions most efficiently, and therefore show an even larger difference in the semimajor axis distributions from the initially smooth simulations than do the lower-mass binaries (bottom panel of Figure 5).

5. A COMPARISON TO NGC 1818

As presented in Li et al. (2013) and discussed in Section 1 in this paper, unlike NGC 1805, the radial distribution of the binary frequency in the LMC star cluster NGC 1818 decreases (only) toward the core. This is intriguing in its own right because older star clusters are consistently observed to have the opposite radial trend in binary frequency, but is even more interesting when compared to NGC 1805, which is also located in the LMC and has the same chronological age, but instead shows a bimodal distribution in binary frequency with radius. Timescale estimates from the observations indicate that the current half-mass relaxation time in NGC 1805 is four to five times shorter than in NGC 1818 (de Grijs et al. 2002). We expand on this discussion below, by comparing our simulations and through simple analytic timescale estimates, to argue that NGC 1818 is less dynamically evolved than NGC 1805, and this can explain the difference in the radial distributions of their binary frequencies.

We re-analyze the two $[Q,\ D] = [0.5, 2]$ simulations of NGC 1818 from Geller et al. (2013b) and compare the results to those of our 20 [0.5, 2] NGC 1805 simulations in the bottom panel of Figure 4. Here we do not plot the distributions of the highest-mass binaries because the uncertainties become so large for the NGC 1818 simulations (due to small sample sizes) that a precise comparison is not possible. First, we find that the overall binary frequency in NGC 1818 is lower. This is due to the higher total cluster mass of NGC 1818, and therefore the higher velocity dispersion, which results in more binaries being disrupted (see also Sollima 2008). More importantly for this discussion, the higher-mass binaries in NGC 1818 have a much lower binary frequency toward the core than in NGC 1805, while there is no such radial trend for the lower-mass binary comparison. Formally, the distribution for highest-mass binaries can be distinguished from those of both the two lowest-mass binary bins at $>3\sigma$ confidence. We interpret this in an analogous way to our interpretation of the middle panel of the same figure; NGC 1818 is less dynamically evolved than NGC 1805 at the same chronological age.

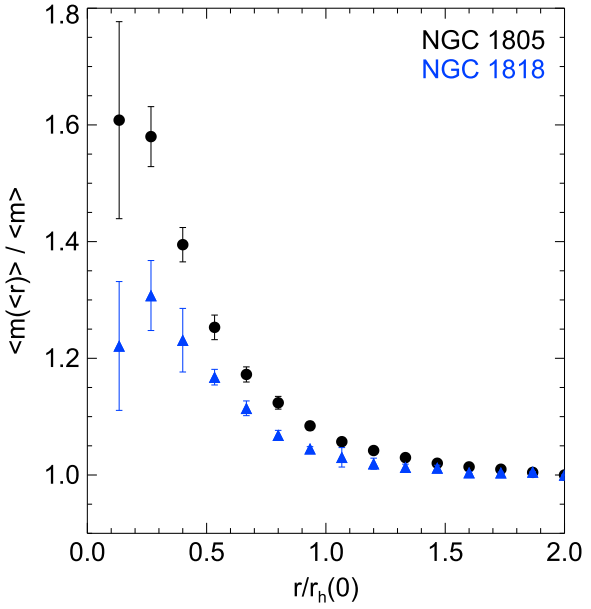

Figure 6. Mass distributions as functions of radius from the respective cluster centers in the NGC 1805 (black circles) and NGC 1818 (blue triangles) models. Each point shows the mean mass inside of the given radius divided by the mean mass of all stars inside of two times the initial half-mass radius, $r_h(0)$, at a time of 30 Myr in the respective model. For both NGC 1805 and NGC 1818, we use the $[Q, D] = [0.5, 2]$ simulations (as we also show in other figures in this paper). The uncertainties for the NGC 1805 points show the standard errors on the means across the 20 individual simulations. For the uncertainties on the NGC 1818 points, we simply show the range in values from the two individual simulations. In constructing this figure, we consider each binary a single object with a mass equal to the sum of the individual component masses.

This difference in dynamical age is also apparent when we compare the radial mass distributions in the NGC 1805 and NGC 1818 models in Figure 6. At the same chronological age of 30 Myr (and for the same $[Q,\ D] = [0.5, 2]$ initial conditions), the radial mass distribution rises more steeply toward the core in the NGC 1805 model than in the NGC 1818 model. Moreover, the NGC 1805 model achieves a higher degree of mass segregation than the NGC 1818 model, within the same cluster lifetime.

This result agrees with simple timescale arguments. For instance, we calculate the initial half-mass relaxation time for stars with masses equal to the mean mass of an object (single or combined mass of a binary) in our NGC 1805 [0.5, 2] model to be about 50 Myr, while for the NGC 1818 [0.5, 2] models a similar calculation yields about 380 Myr (following Spitzer 1987, though the formula does not account for substructure). This result agrees roughly with de Grijs et al. (2002), who estimate from observations that the present-day half-mass relaxation time in NGC 1805 is four to five times shorter than in NGC 1818. Interestingly, a simple estimate of the crossing

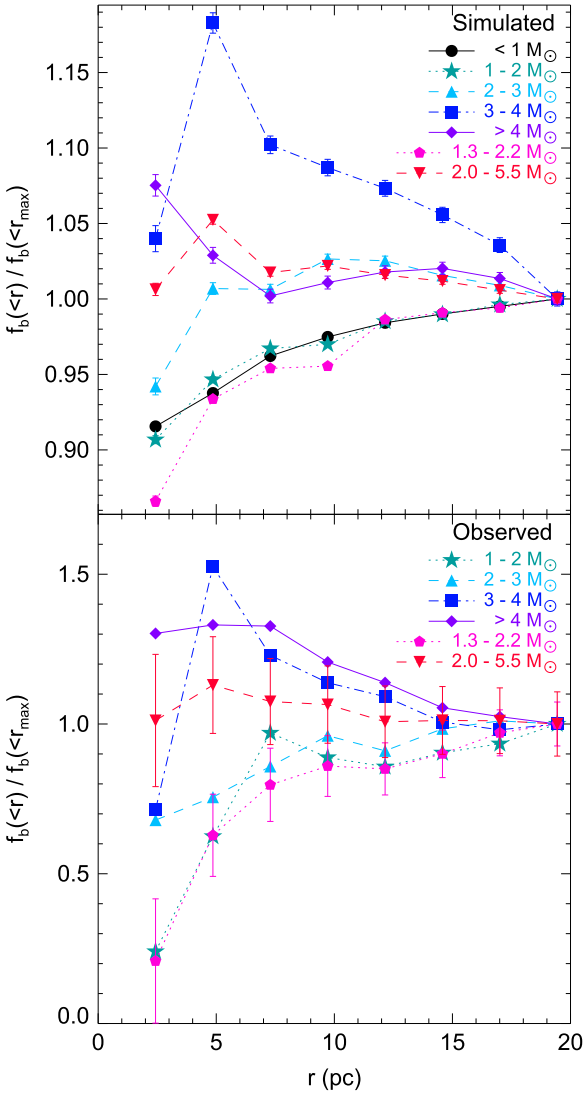

Figure 7. Comparison of the radial distributions of the binary frequency in different mass bins for one simulation of NGC 1818 with $[Q, D] = [0.5, 2]$ from Geller et al. (2013b, top) and the observations from Li et al. (2013, bottom). The different plotting styles for the different mass bins are indicated on each plot. As in Figure 2, we show the binary frequency inside the given radius. We only count binaries with mass ratios $q = m_2/m_1 \geqslant 0.55$, and any binary with $q < 0.55$ is counted as a single star. For the simulation, we use the same 1000 sight lines as in Geller et al. (2013b); the points in the top panel show the means of these values, with uncertainties (visible when larger than the plotted symbols) indicating the standard error on these means. Uncertainties on the observations (derived using Poisson counting statistics, see Li et al. 2013) are much larger, and are shown in the bottom panel for two representative samples for clarity.

time for these two models yields about 5 and 8 Myr, respectively. Thus, the early phase of dynamical disruption, which creates a decreasing trend in binary frequency toward the core, likely operated on a similar timescale in both NGC 1805 and NGC 1818, but the recovery of the binary frequency in the core through mass segregation processes operates $\sim$5–10 times faster in NGC 1805 than in NGC 1818.

We also note that although NGC 1805 may be more dynamically evolved, NGC 1818 still exhibits a similar trend in the radial distribution of the binary frequency as we find in our NGC 1805 models when examining binaries of different mass bins. In Figure 7, we show the result from re-analyzing one of the Geller et al. (2013b) NGC 1818 simulations with $[Q, D] = [0.5, 2]$ (top), compared to the observations of NGC 1818 in the same mass bins. (Unlike NGC 1805, in NGC 1818, the larger number of stars enables us to divide the sample in different mass bins, though the uncertainties are large.) Again, we see that the lowest mass binaries show a decreasing binary frequency toward the cluster core, while moving toward higher-mass binaries shows the trend shifting toward an increasing binary frequency toward the core (in both the observations and simulations).

Finally, the result for NGC 1818 shown in Figure 7, may help to explain the differences between the observations of Li et al. (2013) and Elson et al. (1998), who found opposite trends in the binary frequency as a function of radius. Li et al. (2013) included binaries with primary masses between about 1.3 and 2.2 $M_\odot$, and found a decreasing binary frequency toward the cluster center, while Elson et al. (1998) included binaries with primary masses between 2 and 5.5 $M_\odot$, and found an increasing binary frequency toward the cluster center. We include these mass bins in Figure 7 (both for binaries with mass ratios $\geqslant$0.55) and find different radial trends. We reproduce the observations of Li et al. (2013, as in Geller et al. 2013b) for the lower-mass sample, while the higher-mass binaries of the Elson et al. (1998) sample show a flat, or perhaps marginally increasing, trend in binary frequency toward the core (similar to the conclusions from the N-body models of Elson et al. 1998). de Grijs et al. (2013) and Li et al. (2013) speculated that this difference in binary mass may explain the discrepant observations, and we bolster this argument here. We note that, as stated in Geller et al. (2013b), our NGC 1818 models do not produce as high a binary frequency as observed by Elson et al. (1998, using their observational constraints in our analysis of the simulations). Therefore, we do not perform a more detailed comparison to the observations. We simply offer this discussion as a possible way to reconcile the analyses of Elson et al. (1998) and Li et al. (2013).

6. DISCUSSION

The two rich LMC star clusters NGC 1805 and NGC 1818 are both approximately the same chronological age, but are observed to have two different trends in the radial distribution of their binary frequencies. We found in Geller et al. (2013b) that the radial distribution of the binary frequency can evolve over time from one that decreases toward the core (such as in NGC 1818) to a bimodal distribution (such as in NGC 1805) and eventually to a distribution that increases only toward the core (as observed in many older star clusters). The process occurs on a two-body relaxation timescale, and because NGC 1805 is less massive and more compact than NGC 1818, the expected relaxation time is shorter in NGC 1805. Indeed, de Grijs et al. (2002) estimated from observations that the present-day half-mass relaxation time in NGC 1805 may be four to five times shorter than in NGC 1818. We therefore conjectured in Geller et al. (2013b) that if the binaries in both clusters follow the same evolutionary sequence, the different observed radial trends in the binary frequencies between these two clusters may be further evidence that NGC 1805 is more dynamically evolved than NGC 1818.

We confirm this suggestion here through detailed N-body modeling of NGC 1805. We can reproduce the observations of NGC 1805 through N-body models that draw from *the same* initial binary distributions, fractal dimension, and virial ratio as our NGC 1818 models (which reproduce the observations of

that cluster), with the only differences being the initial masses of the clusters and the initial virial radii. Moreover, our simulations show that both clusters could have formed with binaries drawn from the same parent population, but are observed to be different today because of the clusters' different *dynamical ages* (where dynamical age is the number of relaxation times that the cluster has lived through).

Furthermore, we show above that binaries with different mass primaries undergo this evolutionary sequence of the radial distribution of the binary frequency at different rates, where the higher-mass binaries enter the bimodal and mass segregated phases earlier than the lower-mass binaries (e.g., top panel of Figure 4). This is expected from relaxation time arguments, and we show that this difference can also be used to compare the dynamical ages of clusters, for instance, as we do in the bottom panel of Figure 4. This also highlights the importance of examining binaries in the same mass range when comparing observations across clusters.

As with our NGC 1818 models, we find that our NGC 1805 models that initially have some degree of substructure (here a fractal distribution with dimension $D = 2$) more often match the observed radial trend in binary frequency. We do not attempt to quantify the exact degree or nature of this substructure here. Indeed it is doubtful that such an analysis would be possible, given the available observations, and that the substructure in our models is erased before an age of 30 Myr. Nonetheless, the preference for substructure is encouraging, as this is consistent with observations of star-forming regions (Larson 1995; Cartwright & Whitworth 2004; Kraus & Hillenbrand 2008; Sánchez & Alfaro 2009).

Finally, we note again that, although we focus on an age of 30 Myr for both the NGC 1805 and NGC 1818 models, both de Grijs et al. (2002, and references therein) and Li et al. (2013) find the clusters to have marginally different ages, though these two papers each find a different cluster as being older. Li et al. (2013), who used improved isochrones and performed a more careful field star decontamination, find a nominal age for NGC 1805 of 45 Myr and for NGC 1818 of 18 Myr. This slight difference in age is in the right direction to help increase the expected difference in the radial distributions of the binary frequency in both clusters (though if all else were equal between these clusters, this difference in age on its own would not be enough to produce the different radial trends in binary frequency).

7. CONCLUSIONS

The radial distribution of the binary frequency in a star cluster evolves with time due to dynamical disruptions from close encounters with other stars and mass-segregation processes and can be used to track the dynamical age of a cluster. For a star cluster that is born with wide (soft) binaries, the early evolution of the binaries is dominated by disruptions, which decrease the overall binary frequency and establish a decreasing trend in binary frequency toward the cluster core on approximately a crossing time. The rich LMC star cluster NGC 1818 is observed in this phase of evolution. On a two-body relaxation timescale, dynamical friction and mass segregation effects take over, causing the more massive binaries to sink toward the cluster core, which produces a bimodal radial distribution of the binary frequency. NGC 1805 is observed in this phase of evolution. Later on, as binaries toward the halo also begin to experience the effects of dynamical friction, the binary frequency is transformed into one that only increases toward the core, as is observed in most older star clusters. In Geller et al. (2013b), we showed that this evolutionary sequence can be tracked by looking at binaries of the same mass over time and that the relevant timescale is not necessarily the chronological age, but instead the number of relaxation times the cluster has lived through, which we refer to as the cluster's dynamical age.

We show here that the same evolutionary sequence in the radial dependence of the binary frequency, can be observed at one chronological age for binaries of different primary masses. The higher-mass binaries undergo dynamical friction and mass segregation processes at a faster rate than the lower-mass binaries, and therefore, although all binaries are subject to dynamical disruptions early on, the higher-mass binaries begin increasing their core binary frequency more quickly.

Our detailed *N*-body simulations confirm that NGC 1805 is dynamically older than NGC 1818. Importantly, we can reproduce the observations of both clusters by drawing their stellar populations from the same parent population (though starting from a different total cluster mass and concentration). Furthermore, we show that today's observations of both LMC clusters can be reproduced by drawing their initial binary populations from distributions that are also consistent with observed solar-type binaries in the Milky Way field (Raghavan et al. 2010) and observations of young Milky Way open clusters (e.g., M35, Geller et al. 2010). These results are consistent with a hypothesis that the binaries in NGC 1805 and NGC 1818 were born with similar properties as those in Milky Way clusters, and suggest that binaries may form with similar distributions of orbital parameters and masses within a variety of different environments. We suggest that the radial distributions of the binary frequencies in NGC 1805 and NGC 1818 are different today simply because we are catching them at slightly different stages along a very similar evolutionary sequence.

A.M.G. is funded by a National Science Foundation Astronomy and Astrophysics Postdoctoral Fellowship under Award No. AST-1302765. R.d.G. and C.L. acknowledge partial research funding from the National Natural Science Foundation of China through grant 11373010. A.M.G. also fondly thanks Hannah Jeanne Trouille Geller for allowing him to run and monitor these simulations during her nap times.

REFERENCES

Aarseth, S. J. 2003, Gravitational *N*-Body Simulations (Cambridge, UK: Cambridge Univ. Press)
Adams, F. C., & Myers, P. C. 2001, ApJ, 553, 744
Allison, R. J., Goodwin, S. P., Parker, R. J., et al. 2009, ApJL, 700, L99
André, P., Belloche, A., Motte, F., & Peretto, N. 2007, A&A, 472, 519
Bate, M. R. 2012, MNRAS, 419, 3115
Bressert, E., Bastian, N., Gutermuth, R., et al. 2010, MNRAS, 409, L54
Caballero-Nieves, S. M., Nelan, E. P., Gies, D. R., et al. 2014, AJ, 147, 40
Cartwright, A., & Whitworth, A. P. 2004, MNRAS, 348, 589
de Grijs, R., Gilmore, G. F., Johnson, R. A., & Mackey, A. D. 2002, MNRAS, 331, 245
de Grijs, R., Li, C., Zheng, Y., et al. 2013, ApJ, 765, 4
Elson, R. A. W., Fall, S. M., & Freeman, K. C. 1987, ApJ, 323, 54
Elson, R. A. W., Sigurdsson, S., Davies, M., Hurley, J., & Gilmore, G. 1998, MNRAS, 300, 857
Evans, N. J., II, Dunham, M. M., Jørgensen, J. K., et al. 2009, ApJS, 181, 321
Geller, A. M., Hurley, J. R., & Mathieu, R. D. 2013a, AJ, 145, 8
Geller, A. M., de Grijs, R., Li, C., & Hurley, J. R. 2013b, ApJ, 779, 30
Geller, A. M., & Mathieu, R. D. 2012, AJ, 144, 54
Geller, A. M., Mathieu, R. D., Braden, E. K., et al. 2010, AJ, 139, 1383

Geller, A. M., Mathieu, R. D., Harris, H. C., & McClure, R. D. 2008, AJ, 135, 2264
Ghez, A. M., Neugebauer, G., & Matthews, K. 1993, AJ, 106, 2005
Goodwin, S. P., & Whitworth, A. P. 2004, A&A, 413, 929
Heggie, D. C. 1975, MNRAS, 173, 729
Hole, K. T., Geller, A. M., Mathieu, R. D., et al. 2009, AJ, 138, 159
Hurley, J. R., Pols, O. R., Aarseth, S. J., & Tout, C. A. 2005, MNRAS, 363, 293
Johnson, R. A., Beaulieu, S. F., Gilmore, G. F., et al. 2001, MNRAS, 324, 367
Kaib, N. A., & Raymond, S. N. 2014, ApJ, 782, 60
Köhler, R., Kunkel, M., Leinert, C., & Zinnecker, H. 2000, A&A, 356, 541
Kouwenhoven, M. B. N., Goodwin, S. P., de Grijs, R., Rose, M., & Kim, S. S. 2014, MNRAS, 445, 2256
Kraus, A. L., & Hillenbrand, L. A. 2008, ApJL, 686, L111
Kraus, A. L., Ireland, M. J., Martinache, F., & Hillenbrand, L. A. 2011, ApJ, 731, 8
Kroupa, P. 2001, MNRAS, 322, 231
Küpper, A. H. W., Maschberger, T., Kroupa, P., & Baumgardt, H. 2011, MNRAS, 417, 2300
Lada, C. J., & Lada, E. A. 2003, ARA&A, 41, 57
Larson, R. B. 1995, MNRAS, 272, 213
Li, C., de Grijs, R., & Deng, L. 2013, MNRAS, 436, 1497
Lynden-Bell, D. 1967, MNRAS, 136, 101
Mackey, A. D., & Gilmore, G. F. 2003, MNRAS, 338, 85
McMillan, S. L. W., Vesperini, E., & Portegies Zwart, S. F. 2007, ApJL, 655, L45
Mermilliod, J.-C., Rosvick, J. M., Duquennoy, A., & Mayor, M. 1992, A&A, 265, 513
Milone, A. P., Piotto, G., Bedin, L. R., et al. 2012, A&A, 540, A16
Moeckel, N., & Bonnell, I. A. 2009, MNRAS, 400, 657
Parker, R. J., & Goodwin, S. P. 2012, MNRAS, 424, 272
Patience, J., Ghez, A. M., Reid, I. N., & Matthews, K. 2002, AJ, 123, 1570
Patience, J., Ghez, A. M., Reid, I. N., Weinberger, A. J., & Matthews, K. 1998, AJ, 115, 1972
Peretto, N., André, P., & Belloche, A. 2006, A&A, 445, 979
Plummer, H. C. 1911, MNRAS, 71, 460
Proszkow, E.-M., Adams, F. C., Hartmann, L. W., & Tobin, J. J. 2009, ApJ, 697, 1020
Raghavan, D., McAlister, H. A., Henry, T. J., et al. 2010, ApJS, 190, 1
Sana, H., de Koter, A., de Mink, S. E., et al. 2013, A&A, 550, A107
Sana, H., de Mink, S. E., de Koter, A., et al. 2012, Sci, 337, 444
Sánchez, N., & Alfaro, E. J. 2009, ApJ, 696, 2086
Sollima, A. 2008, MNRAS, 388, 307
Spera, M., & Capuzzo-Dolcetta, R. 2015, arXiv:1501.01040
Spitzer, L. 1987, Dynamical Evolution of Globular Clusters (Princeton, NJ: Princeton Univ. Press)
Tobin, J. J., Hartmann, L., Furesz, G., Mateo, M., & Megeath, S. T. 2009, ApJ, 697, 1103